Somatosensory and Motor Research, September/December 2006; 23(3/4): 111–118

informa
healthcare

Adaptation of trigeminal ganglion cells to periodic whisker deflections

GEORGE FRASER[1], JED A. HARTINGS[2], & DANIEL J. SIMONS[1]

[1]*Department of Neurobiology, University of Pittsburgh School of Medicine, Pittsburgh, PA, USA and* [2]*Department of Applied Neurobiology, Walter Reed Army Institute of Research, Silver Spring, MD, USA*

(Received 22 January 2006; revised 19 March 2006; accepted 25 June 2006)

Abstract
Trigeminal ganglion neurons in adult rats adapt to periodic whisker deflections in the range of 1–40 Hz, manifested as a reduction in spike counts to progressively later stimuli in a train of pulsatile or sinusoidal deflections. For high velocity, pulsatile deflections, adaptation is time- and frequency-dependent; as in the case of thalamic and cortical neurons, adaptation is greater at higher stimulus frequencies. With slower velocity, sinusoidal movements, trigeminal ganglion cells differ from central neurons, however, by exhibiting strong adaptation even at low frequencies. For both types of stimuli, effects in trigeminal ganglion neurons were more pronounced in rats maintained during the recording session under neuromuscular blockade than in non-paralysed animals. Results are consistent with previous findings in other systems that frequency-dependent adaptation of cutaneous primary afferent neurons is affected by mechanical properties of the skin. Such effects are likely to vary depending on the nature of the whisker stimuli and physiological states that affect skin viscoelasticity.

Keywords: *Primary afferent neuron, tactile, somatosensory, vibrissa*

The rodent somatosensory system appears to be highly specialized for the rapid and accurate processing of information arising from deflections of mystacial vibrissae as an animal actively explores its tactile environment. Each whisker hair is anchored within a structurally elaborate and densely innervated follicle containing a variety of mechanoreceptive nerve endings (Rice et al. 1986). Follicles are embedded in an elevated region of skin called the mystacial pad which contains an underlying plexus of muscles whose contraction rotates the base of the follicle to produce whisker protraction (Dörfl 1982). Deflection of the distal end of the hair compresses and stretches tissues within the follicle, and this in turn leads to deformation of nerve endings and the generation of action potentials in the sensory neurons of the trigeminal ganglion. Increasingly, detailed functional studies are revealing the precision and richness of information that the population of first-order neurons potentially conveys to the central nervous system (Szwed et al. 2003; Jones et al. 2004). However, the mechanics of the follicle and of the whisker hair itself have only begun to receive experimental and theoretical attention (Neimark et al. 2003; Mitchinson et al. 2004), though structural bases for some of the physiological properties of the sensory neurons were tentatively identified years ago (Gottschaldt et al. 1971; Lichtenstein et al. 1990).

Recently, we and others have used periodic sensory stimuli to investigate how neural adaptation affects the responses of thalamic and cortical neurons in the main synaptic pathways from the whiskers to the primary somatosensory ''barrel'' cortex. Particularly in thalamocortical circuits, adaptation is highly frequency-dependent, with responses of thalamic and cortical neurons becoming smaller with increasing frequency of whisker stimulation (Garabedian et al. 2003; Castro-Alamancos 2004; Khatri et al. 2004). We were surprised, therefore, to observe that neurons in the brainstem trigeminal principal sensory nucleus (PrV) adapt more strongly to low-frequency whisker deflections than thalamic barreloid neurons (Minnery 2002); the latter's responses appear to be reinforced and augmented by corticothalamic feedback (Minnery and Simons, unpublished observations).

In attempting to account for adaptation effects observed in brainstem neurons, we found that

Correspondence: Daniel J. Simons, Department of Neurobiology, University of Pittsburgh School of Medicine, Pittsburgh, PA 15261, USA. Tel: +1 412 648 9442. Fax: +1 412 648 1441. E-mail: cortex@pitt.edu

ISSN 0899–0220 print/ISSN 1369–1651 online
DOI: 10.1080/08990220600906589

trigeminal ganglion cells themselves become progressively less responsive during a train of repetitive whisker deflections. Because there are no synapses among first-order neurons that could mediate such effects, we reasoned that they are due to physical properties of the whisker follicles and/or the facial tissues in which they are embedded. Responses of rapidly adapting cutaneous receptors are moderately affected by tissue viscoelasticity (Grigg et al. 2004). In the vibrissa system, trigeminal ganglion neurons fire progressively more robustly during the first postnatal month, presumably reflecting changes in the mechanical properties of the facial tissue (Shoykhet et al. 2003), and in adult animals paralyzed by neuromuscular blockade the lack of facial muscle tone often leads to the failure of a deflected whisker to return autonomously to its neutral position following whisker displacement (Minnery and Simons 2003). Here we examine further possible effects of tissue compliance by comparing responses of trigeminal ganglion neurons recorded separately during experiments in which animals were or were not subject to neuromuscular blockade. Results show that response adaptation is stronger and develops more rapidly in paralyzed animals, consistent with an important influence of the viscoelastic properties of the facial tissue itself on the neural response of first-order afferent neurons.

Methods

Surgery and recording conditions

Data are reported from two studies, both of which employed similar surgical preparation which has been described in detail previously (Minnery and Simons 2003) and approved by the Institutional Animal Care and Use Committee of the University of Pittsburgh. Briefly, animals were initially anesthetized with isofluorane or halothane vapors and were subsequently maintained during surgical preparation with 1.5–2.0% halothane or sodium pentobarbital i.v. Anesthetic depth was adjusted continuously to maintain areflexia to foot pinch or surgical manipulation. A tracheotomy was performed, and a polyethylene tube was inserted to maintain an open airway and/or to allow for artificial respiration. A silastic tube was inserted into the external jugular vein for drug delivery, and the femoral artery was catheterized for continuous monitoring of blood pressure. An area of bone several mm^2 overlying the left hemisphere (centered approximately 2.0 mm posterior to bregma and 2.5 mm lateral to the midline) was removed so that recording electrodes could be advanced through the brain into the trigeminal ganglion. A small stainless steel screw was placed in the contralateral frontal bone as an electrical ground. A steel post for holding the head was fixed to the skull using dental acrylic which was also formed into a dam around the craniotomy. All wound margins were sutured closed. During the recording experiment the animal's core temperature was maintained at 37°C using a servo-controlled heating blanket.

Pharmacological conditions during the experiments differed between the two studies. In the first, rats were maintained with pentobarbital sodium (Nembutal,~10 mg/kg/h as needed), and animals breathed spontaneously. Some analyses of data from these animals have been reported previously (Hartings et al. 2003). In the second set of experiments, rats were maintained under light narcosis (fentanyl,~10 μg/kg/h), a regimen used extensively for previous studies of central neurons in our laboratory (see Hartings et al. 2003; Minnery and Simons 2003). For this protocol, animals were paralyzed with pancuronium bromide (1.6 mg/kg/h, i.v.) in order to prevent spontaneous movement of the vibrissae; rats were artificially ventilated using a positive pressure respirator. The sufficiency of ventilation and narcosis was continually measured using a computer program that monitored femoral arterial blood pressure, heart rate, electroencephalogram, and tracheal airway pressure waveform. The latter was used as a monitor of airway patency. No surgical procedures were performed during fentanyl narcosis, and the only sensory stimuli delivered to the animal were small deflections of mystacial vibrissae. Experiments were terminated by an overdose of barbiturate if normative physiological parameters could not be maintained (mean arterial blood pressure of 90–110 mmHg, EEG peak power spectrum 5–10 Hz) or at the end of the recording session, which typically lasted 8–10 h.

Recordings and whisker stimulation

Stainless steel microelectrodes (1–5 MΩ at 1 kHz, FHC, Brunswick, ME) were advanced through the brain into the trigeminal ganglion using a hydraulic stepping microdrive. Whiskers were stimulated manually using a glass probe to generate activity and permit detection of units, which typically lacked spontaneous activity. Once a single unit was isolated, the whisker evoking the response was identified. The whisker hair was trimmed to ~12 mm, and the terminal end was inserted ~2 mm into a multi-angle piezoelectric stimulator. The stimulator was used to deflect the whisker in eight different angular directions (in 45 deg increments relative to the horizontal alignment of the whisker row); deflections consisted of 200 ms ramp-and-hold displacements of 1 mm amplitude and onset and offset velocities of ~125 mm/s. Each angle of deflection was delivered 10 or 20 times, interleaved randomly. Ramp-and-hold stimuli were used to assess each unit's maximally effective direction for delivery of periodic stimuli. Responses evoked during the stimulus

plateau were used for classifying a cell as rapidly or slowly adapting (see below).

In addition to the ramp-and-hold stimuli, whiskers were deflected periodically using two types of displacements (Hartings et al. 2003). In one, brief pulsatile deflections (~10 ms in duration, 700 μm in amplitude with onset and offset velocities of 140 mm/s) were delivered at 1, 2, 4, 8, 12, 16, 20, 30, and 40 Hz. Stimulus trains lasted 4 s for the 1, 2, and 4 Hz stimuli, 2 s for the 8 and 12 Hz stimuli, and 1 s for the 16–40 Hz stimuli. A second protocol employed sinusoidal deflections at the same frequencies. Deflection amplitude was 1 mm and began with the neutral position of the whisker corresponding to the trough of the sine wave. Sinusoidal amplitude was 1 mm peak to peak; sine duration and movement velocity were thus dependent on the frequency of the stimulus. Stimulus waveforms are illustrated in Figure 1. Data are reported for deflections of the whisker in each unit's preferred direction, determined quantitatively using the ramp-and-hold stimuli.

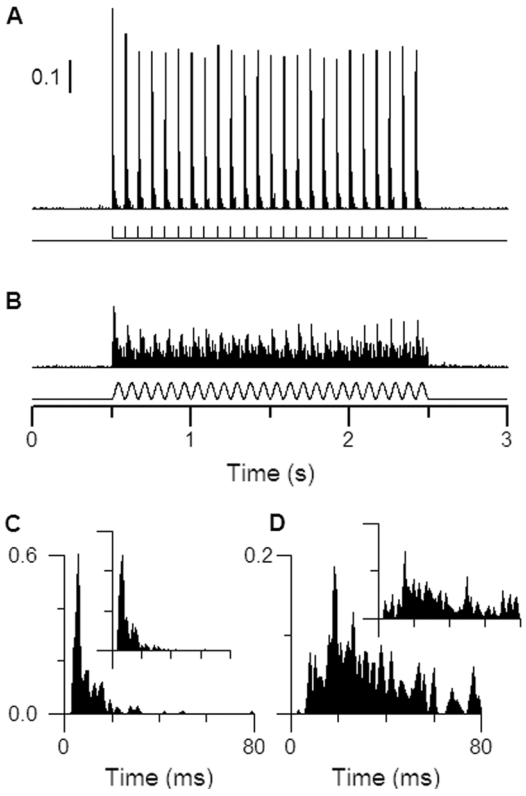

Figure 1. Waveforms of the 12 Hz pulse (A) and sine (B) stimuli, and population neural responses thereof. Population PSTHs are calculated from the 17 cells recorded in the no-paralysis condition and the 22 cells recorded in the paralysis condition. Scale bar in panel A denotes probability of a spike in each 1 ms bin and applies to PSTH in panel B, too. Note that the stimuli are asymmetrical with respect to the hair's resting position; the whisker is deflected from and back to the neutral position. Panels C, D are cycle-time histograms for first-cycle responses to the pulse (C) and sine (B) stimuli; insets show responses accumulated over all subsequent stimulus cycles. Vertical scales denote probability of a spike in each 1 ms bin.

Data acquisition and analyses

Stimuli and data acquisition were performed using an LSI 11/73 computer (Digital Equipment Corp, Maynard, MA) or a PC running LabView (National Instruments, Austin, TX) Spike waveforms were digitized and examined using an amplitude discriminator and oscilloscope equipped with a time delay. Single units were identified on the basis of their waveform shape and amplitude. Sequential spike times were measured with 100 μs resolution and were stored on disk; in later experiments spike waveforms were extracted for offline inspection. Units were classified as rapidly adapting (RA) or slowly adapting (SA) using the ramp-and-hold data. Units which showed significant evoked activity during the plateau period at the maximally effective stimulus angle were classified as slowly adapting; by default, the other units were classified as rapidly adapting (Lichtenstein et al. 1990). Significant discharge during the stimulus plateau was determined by comparing evoked and spontaneous activities using a Student's *t*-test with a significance level of $p = 0.025$.

For analysis of periodic data, peristimulus time histograms (PSTHs) were constructed for each frequency by binning across trials. Adaptation develops over time (stimulus cycles). Therefore, we computed a *final* adaptation index by dividing the mean response in only the last two cycles of the stimulus train by the response in the first cycle (Figure 2). A value of 1.0 indicates no adaptation, whereas values <1.0 reflect proportional reductions in unit firing. To examine the *time course* of adaptation (Figure 3), an adaptation index time-series was computed by dividing the response in each cycle by the response in the first cycle. Each cell's response is thus normalized. In order to estimate the variance in these normalized population values, we computed for the first stimulus in a train the average firing rates of all cells on a trial-by-trial basis and then calculated the mean and standard deviation across trials. The scaling factor needed to normalize this across-cell mean to a value of 1.0 (i.e., no adaptation) was applied to the value of the standard deviation. This normalized standard deviation can be used to set a confidence interval for determining the statistical robustness of the adaptation (one-tailed *z*-score, $p < 0.05$, see Figure 3). Adaptation indices were analyzed using analysis of variance to compare experimental groups, stimulus type, and stimulus frequency. Differences, when observed, were highly robust; therefore, all ANOVA results denoted hereafter as significant were associated with values of $p < 0.001$. Some analyses examined population PSTHs constructed by summing PSTHs from all cells.

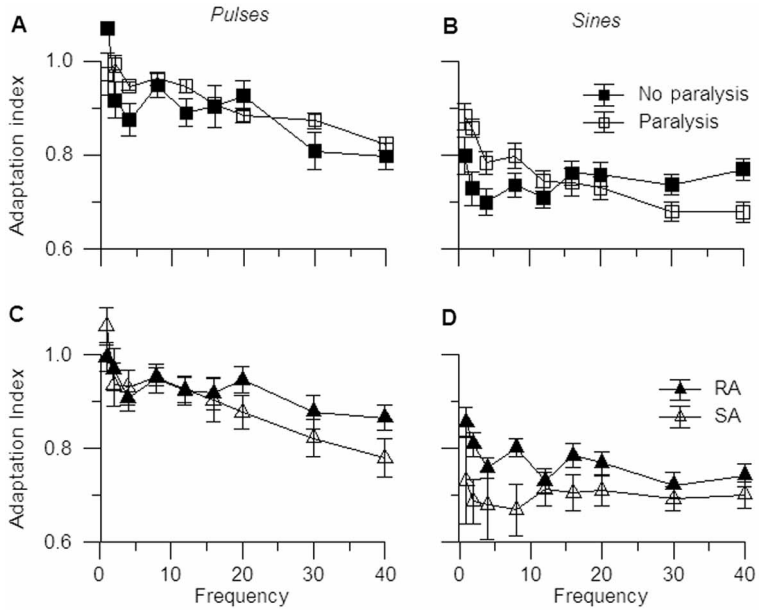

Figure 2. Frequency-dependent adaptation indices for pulsatile (A, C) and sinusoidal (B, D) stimulus trains. Panels A and B plot data obtained from rats in the paralysis ($n = 22$) and no-paralysis ($n = 17$) conditions, respectively. Panels C, D plot data for slowly adapting (SA, $n = 20$) and rapidly adapting (RA, $n = 19$) cells, combined across the paralysis and no-paralysis conditions. Adaptation indices are calculated for each cell by dividing the mean response evoked by the first deflection in a train by the mean response evoked by the last two stimuli in the train. Values <1.0 indicate smaller responses relative to those evoked during the first stimulus cycle.

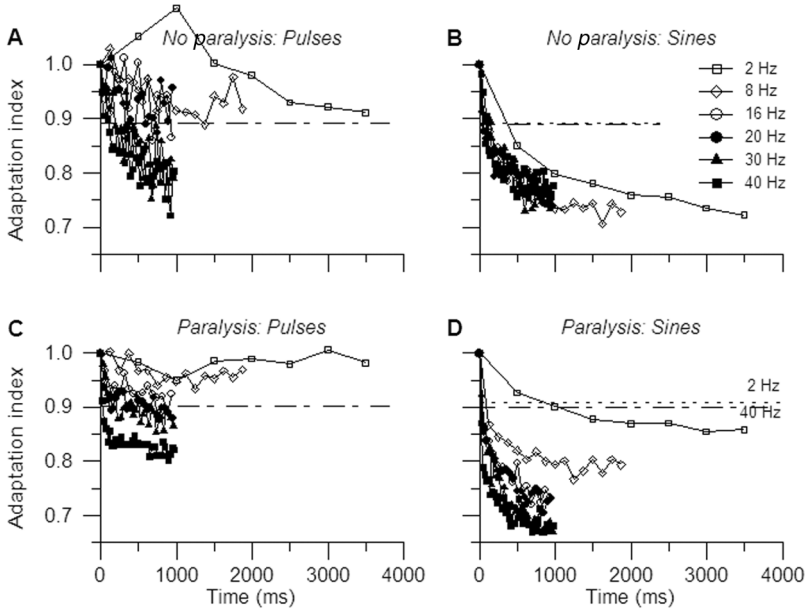

Figure 3. Time course of adaptation as a function of stimulus frequency (symbols) and paralysis state and stimulus type. Adaptation indices were calculated separately for each sequential stimulus within a train; stimulus trains differed in duration depending on frequency. Dashed lines denote confidence limits ($p < 0.05$, see text) calculated from responses to the first stimulus in the 40 Hz train. For sine stimuli, a confidence limit is shown also for the 2 Hz stimulus (dotted line). Data are based on the 17 cells in the non-paralysis condition and 22 cells in the paralysis condition.

We used a vector measure to quantify the temporal distribution of evoked spikes during a stimulus cycle. This was accomplished by treating each stimulus cycle as a circle and calculating a response vector based on the spike counts distributed over 360 deg. The vector phase angle captures the ''center of gravity'' of the response relative to the time course of the stimulus. Vector calculations were taken from population PSTHs and were computed for first cycle responses and for responses accumulated across all other cycles.

Visualization of facial tissue displacement

In one experiment, we examined movement of mystacial pad tissue during whisker stimulation. The rat was anesthetized with halothane and without paralysis. A small flake of aluminum foil, ~0.5 mm diameter, was glued to the face adjacent to the stimulated whisker, which was subsequently deflected using the same periodic stimuli employed during electrophysiological experiments. The stimulator was applied nearer to the face than in other experiments (~5 mm from the skin), in order to provide a displacement of the skin large enough to visualize and measure. Movement of the foil was observed directly using a dissecting microscope and measured under infrared illumination using a photodiode positioned a few mm from the face using a micromanipulator. Measurement was also made of the movement of the stimulator itself using the photodiode circuit (see Simons 1983).

Results

For studies examining the effects of pharmacological paralysis, data are reported from 17 units recorded in 5 barbiturate-anesthetized rats and 22 units recorded in 4 rats maintained during the recording sessions under fentanyl narcosis with neuromuscular blockade. Figure 1 shows population PSTHs for 12 Hz pulses and sinusoids obtained in rats under neuromuscular blockade. For both types of stimuli, responses to the first deflection are largest and decrease with subsequent deflections. Adaptation was greater for the sinusoidal stimuli. For each cell, we calculated a *final* adaptation index quantifying the proportional reduction in responses evoked by the last two stimuli in a train relative to the first (see Methods). Figure 2A, B plots adaptation indices for the two different stimuli and recording conditions as a function of frequency. Adaptation was greater for sinusoidal than pulsatile deflections (ANOVA, $p < 0.001$), and except for sinusoidal deflections in non-paralyzed animals (see below), adaptation was greater at higher frequencies. Pulsatile deflections were accompanied by ~10% reductions in unit firing, reaching a maximum of 20% with 40 Hz stimuli (Figure 2A). By comparison, adaptation indices for sinusoids were 25–30% reduced through most frequencies.

Final adaptation levels for pulses and for sines were similar under paralysis and no-paralysis conditions (Figure 2), and analysis of variance failed to reveal statistically significant differences. The time courses of adaptation differed significantly for the paralysis and no-paralysis conditions, however ($p < 0.001$). For trains of pulsatile deflections, adaptation reached steady-state levels after only a few deflections in paralysed animals, but in non-paralyzed animals responses continued to decrement progressively during the stimulus train, apparently never reaching asymptote (Figure 3A, C). More time was required to achieve steady state for sinusoidal deflections (Figure 3B, D), and this effect was also more pronounced in non-paralysed animals. Particularly in the case of the higher frequency sines (20–40 Hz), which lasted only 1 s, adaptation may not have reached steady state in the non-paralysis condition. The adaptation levels for the 20–40 Hz sines in Figure 2 may therefore be an underestimate of the degree of adaptation. That is, with longer duration stimulus trains, adaptation indices at these frequencies in non-paralyzed rats may be lower and more comparable to those in paralyzed animals.

With sinusoidal stimuli responses in paralysed rats changed temporally. Compared to the first deflection, spikes during the second and subsequent deflections occurred later in the stimulus cycle. This is illustrated by the population cycle-time histograms in Figure 4A, which is based on 10 Hz sinusoidal deflections in the paralysis condition. Note that in the adapted (''other cycles'') response there is a more pronounced peak at approximately $t = 60$ ms, corresponding to deflection offset (return towards origin). A similar effect can be seen for the 12 Hz stimulus in Figure 1D, where the offset response occurs at ~50 ms.

Changes in response timing were quantified by calculating response vectors based on population spike counts distributed over 360 deg of a stimulus cycle (Methods). Figure 4B shows the phase shift computed as the difference in vector phase angle between the first and all other cycles; a larger difference score reflects a greater shift in spike times towards the latter part of the stimulus cycle. In non-paralyzed animals, there was little change in the temporal profile, but in the paralysis condition a strong frequency-dependent effect was observed. Note that with 30 Hz sinusoids, the vector changed ~100 deg, corresponding to a shift in the center of gravity of the spike times by ~8 ms (cycle time = 33 ms). Spike timing shifted towards shorter latencies with the 40 Hz stimulus, which more closely reflects a pulsatile deflection. There were no phase shifts in either condition and at any frequency when the pulsatile stimuli were used (data not shown).

Cells were classified as rapidly or slowly adapting (Methods): 12 RA and 10 SA in the paralysis condition, 7 RA and 10 SA in the non-paralysis condition. Data were normalized to enforce parity in the relative contribution of RA and SA units between conditions. Analysis of variance revealed that in both conditions, cell type had a significant effect on adaptation, with SA units adapting more strongly (Figure 2C, D).

In one experiment in a non-paralysed, halothane-anesthetized rat, movement of the follicle and the surrounding facial tissue was examined visually

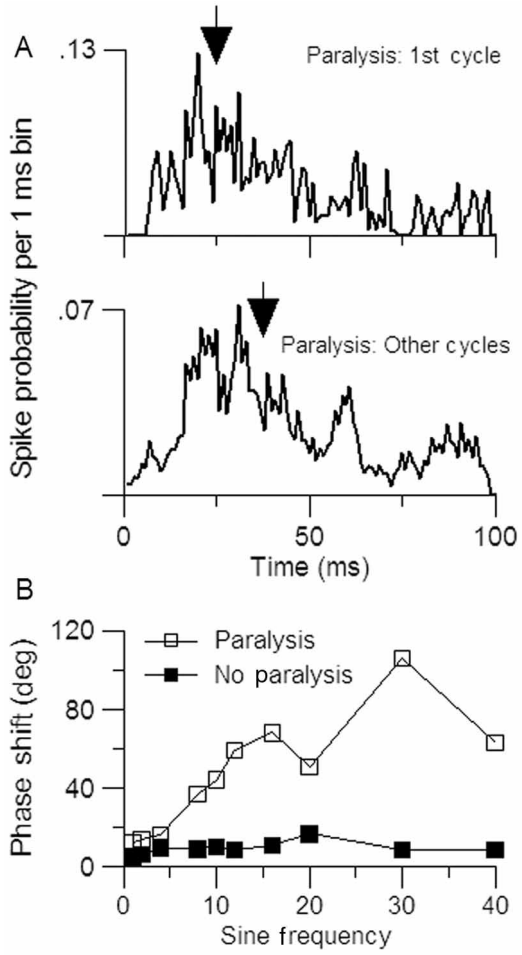

Figure 4. Response phase shift as a function of sinusoid frequency and recording condition. Panel A shows population cycle-time histograms, accumulated for the 22 cells in the paralysis condition, for the first and all subsequent deflections in train of 10 Hz sinusoids. Arrows denote the vector phase angle of each histogram. Graph in panel B plots response phase shifts as a function of frequency and paralysis conditions. Phase shift was computed as the difference in vector phase angle for responses evoked during the first and all subsequent stimulus cycles; a larger phase shift reflects a redistribution of spikes towards the latter part of the stimulus cycle as in (A). Responses to pulsatile stimuli did not display phase shifts in either recording condition, and data are therefore not plotted.

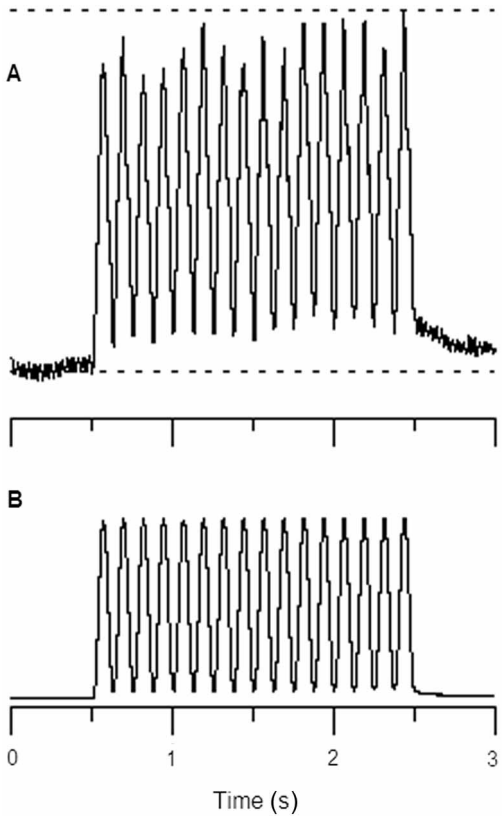

Figure 5. Photodiode measurements of facial tissue (A) and stimulator (B) movement during 8 Hz sinusoidal stimulation. The peak displacement of the stimulator in (B) corresponds to 1.0 mm at 10 mm from the skin; peak amplitude of skin (A) is estimated to be ~0.20 mm. The facial tissue shows progressively increasing displacement as represented by the baseline shift; horizontal lines in (A) are added for clarity. The stimulator shows no such effect (B).

under high magnification during presentation of periodic whisker deflections. Visual inspection suggested that skin at the base of the vibrissal hair was not returning completely to its neutral or undeflected position. Measurements of the movement of the facial tissue using a photodiode (see Methods) confirmed that the skin adjacent to the base of the whisker remained further from origin with each cycle of the stimulus. An example using 8 Hz sinusoidal stimulation is shown in Figure 5A. The baseline position of the skin increased approximately twofold from the end of the first cycle to the start of the last cycle in the train. The stimulator did not quite return to origin during sinusoidal stimulation (Figure 5B), but unlike the skin, it did not show an increasing displacement over time.

Discussion

The present findings demonstrate frequency-dependent adaptation of trigeminal ganglion responses to periodic whisker deflections. Effects were greater for sinusoidal than pulsatile stimuli, and higher frequency stimulation was associated with greater adaptation. For both types of stimuli, effects increased during the stimulus train. Adaptation was greater and its time course was faster in paralysed animals. The observed adaptation effects were somewhat unexpected in light of previous studies in rats, cats, and seals that have observed pronounced, temporally precise entrainment of vibrissa-sensitive primary afferent neurons by repetitive whisker deflection (Dykes 1975; Gottschaldt and Vahle-Hinz 1981; Gibson and Welker 1983; Jones et al. 2004). Indeed, the subset of cells in the present study that were obtained in barbiturate-anesthetized rats

were found to be strongly entrained by pulsatile and sinusoidal stimuli despite the reduction in the number of spikes in successive stimulus cycles (Hartings et al. 2003).

We propose that the adaptation effects observed here reflect the compliance of the facial tissue. At rest and in the absence of a mechanical stimulus, the follicle and the whisker are both in their neutral positions. When the whisker is first deflected with a brief stimulus, for example, a pulse, a large relative displacement is created, causing the whisker hair to compress and stretch tissue in the follicle (see Lichtenstein et al. 1990). With sufficiently long inter-deflection intervals, the follicle and whisker return to their neutral positions. During repetitive deflections, however, the whisker follicle, which is embedded within a compliant mystacial pad, gradually attains an equilibrium position that is displaced from neutral towards the direction of the whisker's deflection. That is, the follicle follows the trajectory of the stimulus but never completely returns to neutral. The whisker hair, on the other hand, returns to its neutral position due to its direct coupling to the mechanical stimulator. Consequently, subsequent deflections of the hair shaft have a smaller amplitude relative to the position of the follicle, exerting less pressure and/or stretching forces on the leading side of the follicle. Responses of the ganglion cells are reduced accordingly, in the present experiments by as much as 30%. For primary afferent neurons innervating primate fingertip, adaptation effects, such as those observed with steady skin indentation, have to date been attributed to mechanical stresses and strains at the scale of the nerve ending, and models have assumed linear or only minimal influence of larger areas of surrounding skin and the underlying bone (Phillips and Johnson 1981; Sripati et al. 2006). Several studies have demonstrated non-linear affects of fingertip viscoelasticity on force patterns evoked by vibrotactile stimuli, including a reduction in force produced during successive stimulus cycles and a non-zero steady-state force level (e.g., Pawluk and Howe 1999); such affects have not yet been examined in the context of neural responses. Progressive reductions in the spike output of cutaneous mechanoreceptors during repeated stimulation have, however, been attributed to stimulus-induced changes in hairy and/or glabrous skin of the cat and raccoon (Tuckett 1978; Pubols 1982).

Tissue compliance could also affect response timing. During a stimulus train the position of the trailing side of the follicle may become progressively more displaced in the direction of the whisker movement. This means that somewhat more force will be applied on that side of the follicle during the return phase of the stimulus cycle. Though the overall response of the cell may be reduced, the relative size of the responses to the initial and return movements of the whisker movement may thus change. This likely accounts for the phase shift observed in paralyzed animals when sinusoidal stimuli were used, including a relatively more pronounced response to the whisker's return towards its neutral position. The present findings thus suggest the need for caution in interpreting stimulation-associated changes in the firing times of central neurons, inasmuch as peripherally related phase shifts in response timing could be attributed erroneously to central neural mechanisms.

Brief, pulsatile whisker deflections are associated with less adaptation than sinusoidal movements, presumably because the whisker (and skin) spends more time at or near origin during a pulsatile stimulus train than during an equivalent frequency sinusoidal stimulus in which the whisker is continuously moving. The shorter deflection times of the pulsatile stimuli likely allow the skin to relax more fully to origin; the movement of the skin is rapid and transient. We found that RA units generally adapt less than SA units. This difference is consistent with previous findings that RA neurons are sensitive to movement, whereas SA neurons are sensitive to both movement and displacement (Shoykhet et al. 2000).

Adaptation to pulsatile stimuli is frequency-dependent due to the shorter inter-pulse intervals in high-frequency stimulus trains. The time available for return decreases with higher frequency pulses, allowing the skin/follicle a shorter time to return to origin. Subsequent pulses impose smaller net displacement upon a follicle and thus evoke a lesser neural response. The frequency dependence of adaptation to sinusoidal stimuli is somewhat different. With sinusoidal stimulation, the whisker is continually moving, and the total time spent at a given displacement is the same regardless of frequency. Sinusoidal stimuli can therefore be expected to evoke comparable levels of adaptation at all frequencies, as observed here except at the very lowest frequencies. We propose that at very low frequencies (less than those used here) the skin/follicle follows the stimulus so closely that little adaptation and response phase shift occurs.

Adaptation was more pronounced and faster in paralyzed animals. Paralysis produced by neuromuscular blockade relaxes muscles in the mystacial pad and elsewhere in the face, thereby rendering the facial tissue more mechanically compliant. Greater pliability of the tissue that surrounds and supports the whisker follicle renders the skin more susceptible to deformation as a result of movement of the whisker hair, leading in turn to more response adaptation. Moreover, steady-state conditions would be reached more quickly. The effects observed here are likely, of course, to reflect the specific features of the whisker deflections, notably that stimuli were unidirectional with respect to the hair's neutral position and that the whisker was

forced back to its neutral position due to the hair's direct coupling to the stimulator. Other types of stimuli, such as those that deflect the whisker symmetrically, are likely to generate different deformations of the facial tissue and hence perhaps different time- and/or frequency-dependent effects. As illustrated by the present findings, systemic physiological conditions also may influence afferent neuron firing inadvertently and unpredictably; we have found, for example, that trigeminal ganglion responses to whisker deflections can be altered by changing central blood pressure (unpublished observations). Whether facial mechanics change also during normal whisking behavior, due for example to muscle fatigue, is unknown. Interpretation of responses of central vibrissa neurons under different experiment/stimulus conditions may thus benefit from parallel assessment of trigeminal ganglion cell activity.

Acknowledgements

We thank Harold Kyriazi, Ebo Kwegyir-Afful, and SooHyun Lee for helpful discussions and comments. This work was supported by NIH NS19950.

References

Castro-Alamancos MA. 2004. Absence of rapid sensory adaptation in neocortex during information processing states. Neuron 41:455–464.

Dörfl J. 1982. The musculature of the mystacial vibrissae of the white mouse. J Anat 135:147–154.

Dykes RW. 1975. Afferent fibers from mystacial vibrissae of cats and seals. J Neurophysiol 53:650–662.

Garabedian CE, Jones SR, Merzenich MM, Dale A, Moore CI. 2003. Band-pass response properties of rat SI neurons. J Neurophysiol 90:1379–1391.

Gibson JM, Welker WI. 1983. Quantitative studies of stimulus coding in first-order vibrissa afferents of rats. 2. Adaptation and coding of stimulus parameters. Somatosens Res 1:95–117.

Gottschaldt KM, Iggo A, Young DW. 1971. Electrophysiology of the afferent innervation of sinus hairs, including vibrissae, of the cat. J Physiol (Lond) 222:60P–61P.

Gottschaldt KM, Vahle-Hinz C. 1981. Merkel cell receptors: Structure and transducer function. Science 214:183–186.

Grigg P, Robichaud R, Prete ZP. 2004. Properties of mouse cutaneous rapidly adapting afferents: Relationship to skin viscoelasticity. J Neurophysiol 92:1236–1240.

Hartings JA, Temereanca S, Simons DJ. 2003. Processing of periodic whisker deflections by neurons in the ventroposterior medial and thalamic reticular nuclei. J Neurophysiol 90:3087–3094.

Jones LM, Lee S, Trageser JC, Simons DJ, Keller A. 2004. Precise temporal responses in whisker trigeminal neurons. J Neurophysiol 92:665–668.

Khatri V, Hartings JA, Simons DJ. 2004. Adaptation in thalamic barreloid and cortical barrel neurons to periodic whisker deflections varying in frequency and velocity. J Neurophysiol 92:3244–3254.

Lichtenstein SH, Carvell GE, Simons DJ. 1990. Responses of rat trigeminal ganglion neurons to movements of vibrissae in different directions. Somatosens Mot Res 7:47–65.

Minnery BS. 2002. The role of trigeminal nucleus principalis in subcortical signal processing. Doctoral Thesis, University of Pittsburgh.

Minnery BS, Simons DJ. 2003. Response properties of whisker-associated trigeminothalamic neurons in rat nucleus principalis. J Neurophysiol 89:40–56.

Mitchinson B, Gurney KN, Redgrave P, Melhuish C, Pipe AG, Pearson M, Gilhespy I, Prescott TJ. 2004. Empirically inspired simulated electro-mechanical model of the rat mystacial follicle–sinus complex. Proc R Soc Lond B 271:2509–2516.

Neimark MA, Andermann ML, Hopfield JJ, Moore CI. 2003. Vibrissa resonance as a transduction mechanism for tactile encoding. J Neurosci 23:6499–6509.

Pawluk DTV, Howe RD. 1999. Dynamic lumped element response of the human fingerpad. J Biomech Eng 12:178–183.

Phillips JR, Johnson KO. 1981. Tactile spatial resolution. III. A continuum mechanics model of skin predicting mechanoreceptor responses to bars, edges and gratings. J Neurophysiol 46:1205–1225.

Pubols BH. 1982. Factors affecting cutaneous mechanoreceptor response. II. Changes in mechanical properties of skin with repeated stimulation. J Neurophysiol 47:530–542.

Rice FL, Mance A, Munger BL. 1986. A comparative light microscopic analysis of the sensory innervation of the mystacial pad. I. Innervation of the vibrissal follicle–sinus complexes. J Comp Neurol 252:154–174.

Shoykhet M, Doherty D, Simons DJ. 2000. Coding of deflection velocity and amplitude by whisker primary afferent neurons: Implications for higher level processing. Somatosens Mot Res 17:171–180.

Shoykhet M, Shetty P, Simons DJ. 2003. Protracted development of responses to whisker deflection in rat trigeminal ganglion neurons. J Neurophysiol 90:1432–1437.

Simons DJ. 1983. Multi-whisker stimulation and its effects on vibrissa units in rat SmI barrel cortex. Brain Res 276:178–182.

Sripati AP, Bensmaia SJ, Johnson KO. 2006. A continuum mechanical model of mechanoreceptive afferent responses to indented spatial patterns. J Neurophysiol 95:3852–3864.

Szwed M, Bagdasarian K, Ahissar E. 2003. Encoding of vibrissal active touch. Neuron 40:621–630.

Tuckett RP. 1978. Response of cutaneous hair and field mechanoreceptors in cat to paired mechanical stimuli. J Neurophysiol 41:150–156.